Kinetics of microdomain structures in multi-phase polymer-liquid crystalline materials

S. K. Das[*], A. D. Rey[**]

Department of Chemical Engineering, McGill University
3610 University Street, Montreal, Quebec H3A 2B2, Canada.
[*]susanta.das@staff.mcgill.ca
[**]alejandro.rey@mcgill.ca

ABSTRACT

A mesoscopic kinetic model for phase separation in the presence of liquid crystalline order has been formulated, and solved using high performance numerical methods. The thermodynamic phase diagram on temperature-polymer concentration plane indicates the presence of coexistence regions between isotropic and liquid crystalline phases. These regions are itself partition by the phase separation spinodal and the phase ordering spinodal. We characterize the morphologies following temperature quenches in the phase diagram. The scenario is completely different from isotropic mixing since the continuous phase exhibits liquid crystalline ordering. Microdomains of the dispersed phase induce long- and short-range forces affecting the kinetics of the separation and the emerging structures. Presence of topological defects and elastic distortions around the microdomains formed during the phase separation dominate the morphology. The free energy of the system establishes dynamics and correlations of the morphological structures.

Keywords: multiphase, phase separation, microdomain structures, topological defects, phase diagram

1 INTRODUCTION

Multiphase polymer-liquid crystal blends are new multifunctional materials with unique electro-optical properties. The formation process is driven by thermodynamic instabilities, and the emerging microstructures reflect the curvature elasticity of the liquid crystalline phase. Such multiphase polymer dispersed liquid crystal (PDLC) makes a new composite material with unique physical properties that originate from the orientational ordering of the liquid crystal. Mechanical and electro-optical properties of this system are primarily determined by the collective behaviors of these binary mixtures. Because when flexible polymers are introduced into LC's the electro-optical properties of the system are considerably affected due to the deformation of the nematic director field, which can result in nontrivial collective behaviors, leading to the formation of spatially modulated structures. Depending on the time scale that controls these processes, a rich variety of morphologies have been observed [1-2]. Phase separation of such systems can be induced either through a thermal quench [3-4] or through polymerization [5]. Because of the number of nonequilibrium processes involved, however, there is a little theoretical understanding of the factors that control the domain morphology. A Cahn-Hilliard framework that allows composition and orientational density to evolve in a coupled fashion as functions of position and time following a temperature quench was performed [3]. Their framework includes the orientational density's second-order tensorial nature [6] where free energy of the system contains orientational density's three term gradient expansions. But details morphological structures, especially the free energy profiles of the system, characterization of morphological structures, phase separation and phase transition mechanism, topological defect structures, etc., remain unclear yet.

In this paper we present a nonlocal dynamical model focusing on the interplay between phase-separation and phase ordering kinetics in mixtures of short, liquid crystals (rigid rods) and long, flexible polymers, as a first step towards the rational design and control of the microdomain morphology. Here we consider fully nonlocal model without resorting to the three term gradient expansions of Landau-type [6] while derived free energy of the system. Computationally, this is challenging because it would require evaluating multiple convolutions at each moment in time. The advantage of our system is that we can calculate two order parameters (conserved and non-conserved) solving two coupled time-dependent equations together from a microscopic model of polymers and liquid crystals without loosing any information of order parameters.

2 MODEL FORMULATION

2.1 Thermodynamic phase diagram

In this section we represent the free energy to construct the static phase diagrams. According to [7], the free energy density of polymer-liquid crystal mixtures can be written as;

$$f(\varphi, S) = \beta \Delta F_{mix}/N_T = f^{(i)} + f^{(n)}, \qquad (1)$$

$$f^{(i)} = \frac{\varphi_I}{n_I} \ln \varphi_I + \frac{\varphi_A}{n_A} \ln \varphi_A + \chi \varphi_I \varphi_A , \qquad (2)$$

$$f^{(n)} = \frac{1}{2}\left(\frac{\Gamma_0}{n_A}\right)\varphi_A^2 S^2 - \frac{\varphi_A}{n_A} \ln\left(\frac{I_0\left(\Gamma_0 \varphi_A S\right)}{2}\right) , \qquad (3)$$

$$\varphi_I + \varphi_A = 1 , \; \Gamma_0 = \left(\chi_a + 5/4\right) n_A , \; \beta = 1/k_b T , \qquad (4)$$

$$I_0\left(\Gamma_0 \varphi_A S\right) = \int_{-1}^{1} \exp\left(\frac{3}{2}\Gamma_0 \varphi_A S\left(x^2 - \frac{1}{3}\right)\right) dx , \qquad (5)$$

where T is the absolute temperature, k_b is the Boltzmann constant, S is the 'scalar' orientational order parameter of the liquid crystals, χ is the Flory-Huggin's interaction parameter, the terms χ_a and $(5/4)n_A$ in Γ_0 indicates the orientation-dependent attractive interactions between the mesogens and excluded volume interactions between mesogenic molecules respectively, n_I and n_A are the number of segments on the isotropic (monomer or polymer) component and the number of segments (axial ratios) on the mesogen respectively, and φ_I and φ_A are the corresponding volume fractions, respectively. The first two terms in the right hand side of equation (2) represent the entropy of mixing. For thermodynamical reasons, the entropy of mixing must be dominant at high temperatures and so we can introduce the temperature parameter, τ, defined by $1/\tau = \chi = U_0/k_b T$, where U_0 controls the miscibility of the two species in the isotropic phase. The two terms on the right side of equation (3) represent the free energy change due to the alignment of the liquid crystals.

Fig. 1 Phase diagram of the binary mixtures of polymer and liquid crystals on the temperature–concentration plane for $n_I = 25$, $n_A = 2$, $\alpha = 2.5$.

As shown by De Gennes and Prost [6] equations (1-5) predicts the emergence of a stable nematic phase when $\Gamma_0 \varphi_A = 4.55$. Using the following definitions:

$$\Gamma_0 = \left(\chi_a + 5/4\right) n_A , \; \alpha = \chi_a / \chi , \; \chi = 1/\tau , \qquad (6)$$

where $\alpha = \chi_a / \chi$ represents the relative strength of interactions, and τ is the reduced temperature, it is found

that the threshold $\Gamma_0 \varphi_A = 4.55$ gives the following concentration dependence of the reduced nematic-isotropic transition (NIT) temperature:

$$\tau_{NI}\left(\varphi_A\right) = \frac{\alpha n_A \varphi_A}{4.55 - 1.25 n_A \varphi_A} . \qquad (7)$$

For simplicity, we denote the isotropic component composition, φ_I, by ϕ $\left(\phi \equiv \varphi_I\right)$ in the phase diagram (Fig 1).

2.2 Kinetic equations

The dimensionless total free energy of the system consists of the bulk free energy and a nonlocal free energy that controls the cost of gradients in composition and orientational density, in the absence of surface terms and external fields, can be expressed as [8]

$$\tilde{F} = \tilde{T} \times \oint_{\tilde{v}} \left(\tilde{f}^h + \frac{1}{\tilde{T}} \tilde{f}^g \right) d\tilde{v} , \qquad (8)$$

$$\tilde{f}^h = \left[\frac{\tilde{\varphi}}{n_I} \ln \tilde{\varphi} + \frac{\left(1-\tilde{\varphi}\right)}{n_A} \ln\left(1-\tilde{\varphi}\right) + \chi \tilde{\varphi}\left(1-\tilde{\varphi}\right) \right.$$
$$\left. + \frac{3}{4}\left(\frac{\tilde{\Gamma}_0}{n_A}\right)\left(1-\tilde{\varphi}\right)^2 \tilde{Q} : \tilde{Q} - \frac{\left(1-\tilde{\varphi}\right)}{n_A}\ln\left(\frac{\tilde{I}_0}{2}\right) \right] , \qquad (9)$$

$$\tilde{f}^g = \left[\frac{1}{2\tilde{D}}\times\left(\tilde{\nabla}\tilde{\varphi}\right)^2 + \frac{\tilde{R}}{\tilde{D}}\times\left(\tilde{\partial}_i \tilde{\varphi}\right)\left(\tilde{\partial}_j \tilde{Q}_{ij}\right) \right.$$
$$\left. + \frac{\tilde{G}}{2\tilde{D}}\times\left(\tilde{\partial}_k \tilde{Q}_{ij}\right)^2 + \frac{\tilde{P}}{2\tilde{D}}\times\left(\tilde{\partial}_i \tilde{Q}_{ik}\right)\left(\tilde{\partial}_j \tilde{Q}_{jk}\right) \right] , \qquad (10)$$

where

$$\tilde{I}_0 = \int_0^{2\pi}\int_0^{\pi} exp\left[\frac{3}{2}\tilde{\Gamma}_0\left(1-\tilde{\varphi}\right)\tilde{Q}:\left(\sigma\sigma - \frac{\delta}{3}\right) \right.$$
$$\left. sin^2\theta d\theta d\omega \right] . \qquad (11)$$

The dimensionless governing equations of the system becomes [8]

$$\frac{\partial \tilde{\varphi}}{\partial \tilde{t}} = \left[\tilde{D}\times\tilde{T}\times\tilde{\nabla}^2\left(\frac{\partial \tilde{f}^h}{\partial \tilde{\varphi}}\right) - \tilde{\nabla}^4\tilde{\varphi} - \tilde{R}\times\tilde{\nabla}^2\left(\tilde{\nabla}\cdot\tilde{\nabla}\tilde{Q}\right) \right] , \qquad (12)$$

$$\left[\frac{\partial \tilde{Q}}{\partial \tilde{t}}\right]^{[s]} = \left[-\tilde{T}\times\tilde{D}\times\tilde{E}\times\frac{\partial \tilde{f}^h}{\partial \tilde{Q}} + \tilde{E}\times\tilde{R}\times\tilde{\nabla}\cdot\tilde{\nabla}\tilde{\varphi} \right.$$
$$\left. + \tilde{E}\times\tilde{G}\times\tilde{\nabla}^2\tilde{Q} + \tilde{E}\times\tilde{P}\times\tilde{\nabla}\left(\tilde{\nabla}.\tilde{Q}\right) \right]^{[s]} \qquad (13)$$

where $\tilde{t}$ is the dimensionless time, $\tilde{D}$ is the dimensionless diffusion parameter, $\tilde{E}$ is the phenomenological constant, $\tilde{R}$ is the coupling parameter, $\tilde{G}$, and $\tilde{P}$ represents dimensionless Frank elastic parameters respectively and

$\tilde{Q}$ is a second rank symmetric and traceless tensor [9]. Dimensionless Eqs. (8)-(13) are solved by a high performance numerical scheme with periodic boundary condition [8].

3 RESULTS AND DISCUSSIONS

A typical phase diagram of the system on the temperature-
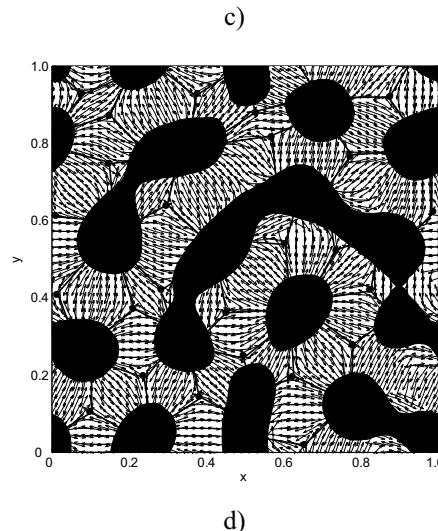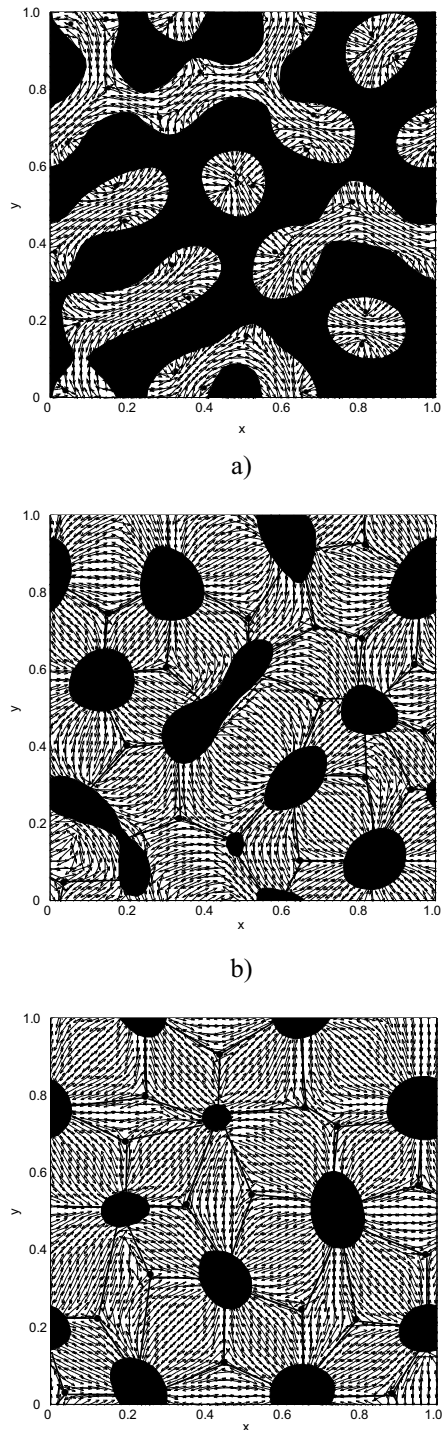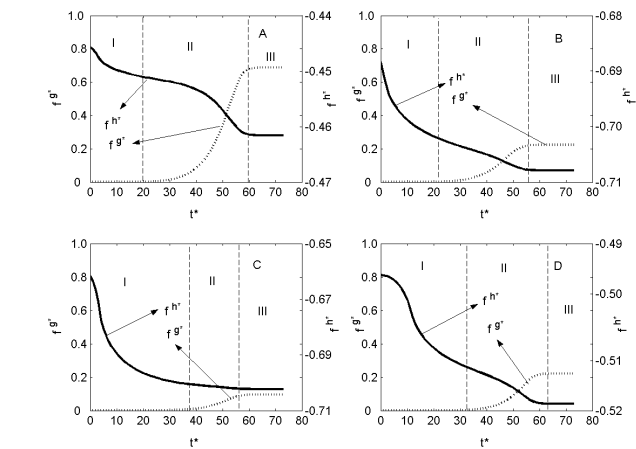

a)

b)

c)

d)

Fig. 2 Snapshot of the local composition of the system at a late time step following a quench to; a) point A, b) point B, c) point C and d) point D for $n_I = 25$, $n_A = 2$, $\alpha = 2.5$, $\tilde{D} = 1000$, $\tilde{E} = 1.0$, $\tilde{R} = 0.2$, $\tilde{G} = 0.1$, and $\tilde{P} = 0.1$. Black corresponds to isotropic polymer and white corresponds to pure liquid crystals (LCs). The arrows represent the local nematic director, and defects are marked with small solid circles.

Fig. 3 Free energy profiles of the system following a quench to; a) point A, b) point B, c) point C and d) point D for $n_I = 25$, $n_A = 2$, $\alpha = 2.5$, $\tilde{D} = 1000$, $\tilde{E} = 1.0$, $\tilde{R} = 0.2$, $\tilde{G} = 0.1$, and $\tilde{P} = 0.1$. Dimensionless homogeneous energy, f^{h^*}, Dimensionless gradient energy, $f^{g^*} = 325 \times \tilde{f}^g$, and Dimensionless time, $t^* = 10^5 \times \tilde{t}$.

concentration plane is shown in Fig. 1 which is computed with $n_I = 25$, $n_A = 2$, and $\alpha = 2.5$. In the figure, ϕ, denotes the isotropic component composition (polymer concentration). The coexistence (binodal) curve of the phase equilibrium is derived by a double tangent method.

Details procedure for computing binodal and spinodal curves for such a system is documented in the work [8]. We study the morphology following four quenches from the isotropic, homogeneous phase into the isotropic-nematic (IN) coexistence region below the triple point line. Four regions are indicated by filled circles and denoted by points A, B, C and D respectively in the phase diagram (Fig. 1).

Fig. 2 represents the snapshot of compositional order of the system at points A, B, C and D respectively. In Fig. 2(a), mass matrix phase is isotropic and droplet phase is nematic. In Fig. 2(a) we can see that a pair of topological defects forms inside each microdomain due to the presence of repulsive Peach-Koehler forces. In our system the repulsive force naturally arises from interaction via the elastic deformation of liquid crystal [1]. We can see from the Fig. 2(a) that orientation inside the droplet is perpendicular implying strong normal anchoring of liquid crystal molecules at the droplet boundary. Nematic droplets must develop defects because the LCs wants to be parallel to each other and parallel to the droplet interface too. This result agrees quite well with the results reported by Lapena *et.al* [3] (see Fig. 3, [3]). In Fig. 2(b)-2(d), mass matrix phase is nematic and microdomain phase is isotropic. In Fig. 2(b)-2(d), isotropic microdomains suspended into the nematic matrix are surrounded by the topological defects. One interesting feature of the defect lattice is its topology. Solid lines represent the interconnection between defect cores and isotropic microdomains. Defect structures form cellular polygonal networks that are mostly four-sided and the side of each polygon ends either at the droplet or at another defect. Most of the defects are +1/2 disclinations. Some of them are +1 disclinations which eventually split into two +1/2 disclinations as can be seen from Fig. 2(b) and 2(c). In the case of point C (see Fig. 2(c)), microdomians are almost positionally ordered whilst they form fabrillar networks for the case of point D (see Fig. 2(d)).

To get better understanding of underlying physics in phase separation processes, we calculated free energy profiles at each of the quenching positions of the system. Fig. 3 represents the dimensionless homogeneous and gradient energy as a function of dimensionless time following quenches to the point A, B, C and D. In Fig. 2, we can clearly see three distinct regimes, namely initial time lag regime (I), growth/relaxation regime (II) and the plateau regime (II). In the II regime, the free energy shows growth in the gradient energy and decrease in homogeneous energy indicating that phase separation and phase ordering spinodal decomposition (SD) drives the system to be unstable, leading to the breakdown of the interconnected domains and formation of isotropic microdomains or fabrillar networks. In the crossover regime III, a plateau regime corresponding to the onset of the breakdown of the interconnected structure (see Fig. 2) appears. The plateau is quite pronounced in both of the energy profiles, which indicates that phase separation get saturated and signals a transition from early stage to intermediate stage of phase separation.

4   CONCLUSION

A nonlocal mesoscopic dynamic model for multiple phase separation, based on a tensor theory, in the presence of liquid crystalline order has been formulated, and solved using high performance numerical methods. We characterized the emerging morphologies following four temperature quenches into the physically meaningful regions of phase diagram. Phase separations from temperature quenches of isotropic binary mixtures start with the formation of small domains that grow and coarsen as time elapses which leads to polydisperse dispersions of growing microdomains that eventually phase separate macroscopically. It has been found that ordering dramatically affects morphology. Topological defects arise due to the elastic distortions around the microdomains formed during the phase separation. Defect structures form cellular polygonal networks that are mostly four-sided and the side of each polygon ends either at the droplet or at another defect. The free energy of the system establishes the dynamics and correlation of the morphological structures. Formation of interconnected (bicontinuous) networks or microdomins depends on whether ordering or phase separation is the initially dominant process. Compared to the experimental and numerical results available in the literature, our simulation results may able to provide new insights into the understanding of new emerging microdomain tropological defect morphology in liquid crystalline materials.

REFERENCES

[1] J.W. Doane, Liquid Crystals: Applications and Uses, ed. B. Bahadur, World Scientific, NJ, 1990.

[2] P.S. Drzaic, Liquid crystal dispersions, World Scientific, Singapore, 1995.

[3] A.M. Lapena, S. C. Glotzer, S. A. Langer, and A.J. Liu, Phys. Rev. E 60(1), R29, 1999.

[4] M. Graca, S. A. Wieczorek, and R. Holyst, Macromolecules, 36, 6903-691, 2003.

[5] G.P. Crawford and S. Zumer, Liquid Crystals in Complex Geometries Formed by Polymer and Porous Networks, Taylor & Francis, London, 1996.

[6] P. G. de Gennes and J. Prost, The Physics of Liquid Crystals, Oxford University Press, NY, 1993.

[7] S. K. Das and A. D. Rey, Computational Modelling of Multi-Phase Equilibria of Mesogenic Mixtures. J. Comp. Mat. Sci. 2003, (In Press).

[8] S. K. Das and A. D. Rey, A nonlocal dynamic model of multi-phase inhomogeneous mixtures of flexible polymer and liquid crystal materials, J. Chem. Phys., 2003, (to be appear).

[9] A.D. Rey and T. Tsuji, Macromol. Theory Simul. **7**, 623-639, 1998.